

Giant magnetoresistance in the intermetallic compound Mn_3GaC

K. Kamishima,* T. Goto, H. Nakagawa,[†] N. Miura, M. Ohashi, and N. Mori
Institute for Solid State Physics, University of Tokyo, Kashiwa, Chiba 277-8581, Japan

T. Sasaki and T. Kanomata

Faculty of Engineering, Tohoku-Gakuin University, Tagajo, Miyagi 985-8537, Japan

(Received 25 January 2000; revised manuscript received 7 June 2000; published 20 December 2000)

We have measured the transverse resistance of an intermetallic compound Mn_3GaC in pulsed high magnetic fields up to 25 T. Giant magnetoresistance is observed due to the field-induced magnetic transition from the antiferromagnetic to the intermediate phase at low temperatures. The temperature dependence of magnetoresistance shows a dip at the Curie temperature. The dip can be explained using a simple model of de Gennes and Friedel based on magnetic critical scatterings. The normal Hall coefficient is found to show a striking change at the transition, suggesting that the giant magnetoresistance is caused by the change of the carrier concentration.

DOI: 10.1103/PhysRevB.63.024426

PACS number(s): 72.80.Ga

I. INTRODUCTION

Ternary manganese compounds with a formula Mn_3MX ($M = \text{Ga}, \text{Al}, \text{Zn}, \text{In}, \text{and Sn}$; $X = \text{N and C}$) have a cubic crystal structure of perovskite type. The magnetic Mn atoms are located at the face-centered positions, the M atoms at the cubic corners, and the X atoms at the body-centered positions. In spite of the simple crystal structure, these compounds show a wide variety of magnetic moments, structures, and transitions.^{1,2}

Mn_3GaC exhibits complicated magnetic phase transitions. In a previous paper,³ we reported results of magnetization measurements of Mn_3GaC . The ground state of Mn_3GaC is antiferromagnetic at ambient pressure. At higher temperatures, it exhibits a transition to an intermediate phase with an abrupt decrease in volume at $T_{\text{AF-I}} = 160.1$ K. With increasing the temperature further, a transition to a ferromagnetic phase is observed at $T_{\text{I-F}} = 163.9$ K and to a paramagnetic phase at $T_{\text{C}} = 245.8$ K. The Curie temperature T_{C} is determined by the conventional Arrott plot. The transition between the antiferromagnetic and the intermediate phase is of first order and the other transitions are of second order. Mn_3GaC exhibits a metamagnetic transition from the antiferromagnetic to the intermediate phase accompanied by magnetization hysteresis at low temperatures.³ The feature of the sharp transition does not change with temperature, although the transition field decreases with increasing temperature. It is quite different from the ordinary magnetic transition observed in antiferromagnets with localized magnetic moments. We show in Fig. 1 the magnetic phase diagram, which is determined in the temperature-field plane.

In the antiferromagnetic and ferromagnetic phases, the Mn moments in a (111) plane are uniform along the [111] direction.⁴ The ferromagnetic (111) planes alternate along the [111] direction in the antiferromagnetic phase. The magnitude of the Mn moment μ_{Mn} is estimated to be $1.8\mu_{\text{B}}$ at 4.2 K in the antiferromagnetic phase and $1.2\mu_{\text{B}}$ at 170 K in the ferromagnetic phase. The intermediate phase has a canted ferromagnetic structure that is possibly the same as that of Mn_3ZnC and $\text{Mn}_3\text{GaC}_{0.935}$.⁵ However, in both the ferromag-

netic and antiferromagnetic states, the Mn moment μ_{Mn} is much lower than those of $3\mu_{\text{B}} - 4\mu_{\text{B}}$ observed in many manganese intermetallic compounds. The volume decrease observed at $T_{\text{AF-I}}$ would be related with the reduction of the Mn moment at the transition.

In order to investigate the relation between magnetic states and transport properties, we have measured the transverse magnetoresistance of Mn_3GaC in pulsed high magnetic fields and the Hall resistance in steady magnetic fields.

II. EXPERIMENTAL PROCEDURE

Polycrystalline samples of Mn_3GaC were prepared by a direct reaction of the constituent elements. We employed gallium ingots of 4N purity, carbon fine powder of 11N purity, and the manganese grains of 4N purity, which were degassed before the synthesis. The manganese grains and the gallium ingots were mixed in the desired proportions of 3.00 and 1.00, respectively. The carbon fine powder was added to them in the excess proportion of 1.05 in order to avoid the formation of carbon vacancies. They were sealed in an evacuated silica tube whose inner surface was coated with carbon. The vacuum degree was about 10^{-6} Torr. The sealed tube was heated to 800 °C for 7 days in an electric furnace.

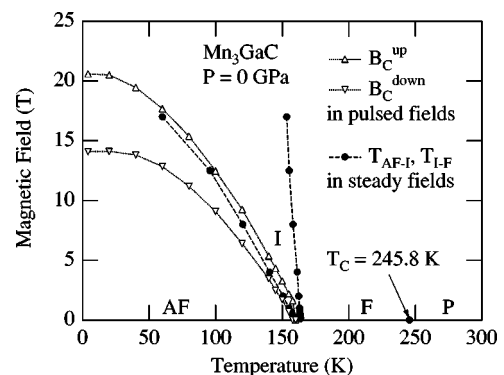


FIG. 1. Magnetic phase diagram of Mn_3GaC in the temperature-field plane.

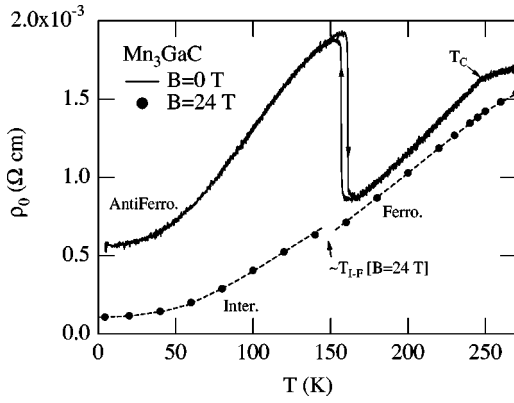


FIG. 2. ρ - T curves of Mn_3GaC at zero field (solid line). The markers are at $B=24$ T. Dashed lines are drawn through the markers for clarity.

After quenching the tube, the product was removed from the tube and crushed into fine powder. Furthermore, we annealed it again under the same conditions, because one procedure did not homogenize the sample perfectly. Differently, the magnetic transitions would become broad due to its very sensitive properties versus the chemical formula. A very small amount of carbon powder remained in excess after the synthesis but had almost no effect on the magnetic and transport measurements. From the preparation processes, δ in $\text{Mn}_3\text{GaC}_{1-\delta}$ had to be extremely close to 0.00. The prepared sample exhibited very sharp transitions, as reported previously,³ which indicates that the quality and the homogeneity of the sample were good.

The sintered polycrystals were cut into a bar shape for transport measurements and into thin slices for Hall resistance measurements. The transverse resistance and Hall resistance measurements were carried out by the standard four-probe method with a dc current perpendicular to magnetic fields. In the former case, we produced pulsed magnetic fields up to 25 T with a duration time of about 10 ms, by using a nondestructive long pulse magnet.⁶ In the latter, we used a superconducting magnet that scans magnetic fields between -5 and 5 T. By reversing magnetic fields, the diagonal component of the resistivity was eliminated from the Hall resistance signal.

III. EXPERIMENTAL RESULTS

The temperature dependence of transverse resistivity ρ of Mn_3GaC is shown in Fig. 2. Abrupt change in resistivity is observed at the transition between the antiferromagnetic and intermediate phases. Except for the hysteresis region of the transition, the ρ - T curves coincide in the processes of increasing and decreasing temperature. The Curie temperature T_C of this sample is 246 K, determined from the change of slope in the ρ - T curve. The value of T_C is consistent with that determined by the previous magnetization measurements.

Figure 3 shows the transverse magnetoresistance of Mn_3GaC in pulsed high magnetic fields. The metamagnetic transition takes place below $T_{\text{AF-I}}$ and the resistivity changes

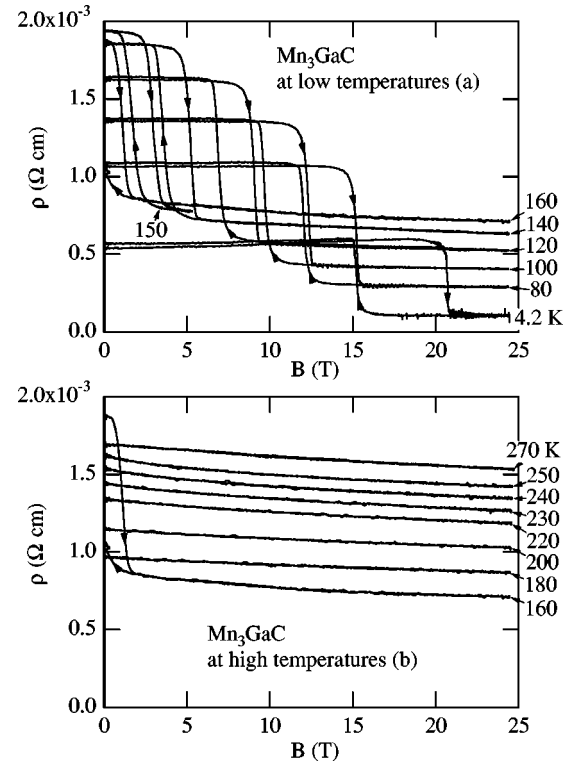


FIG. 3. Transverse magnetoresistance of Mn_3GaC in pulsed high magnetic fields.

abruptly at the transition fields. With increasing temperature, the absolute value of the change $\Delta\rho$ increases but the relative value $\Delta\rho/\rho$ decreases. In the ferromagnetic and paramagnetic phases, ρ decreases slowly with increasing magnetic field. The magnetoresistance shows a dip in the vicinity of T_C (see Fig. 4).

The temperature dependence of ρ at $B=24$ T is shown in Fig. 2 to better understand the above experimental results of magnetoresistance. We can see the giant magnetoresistance due to the metamagnetic transition at low temperatures, and

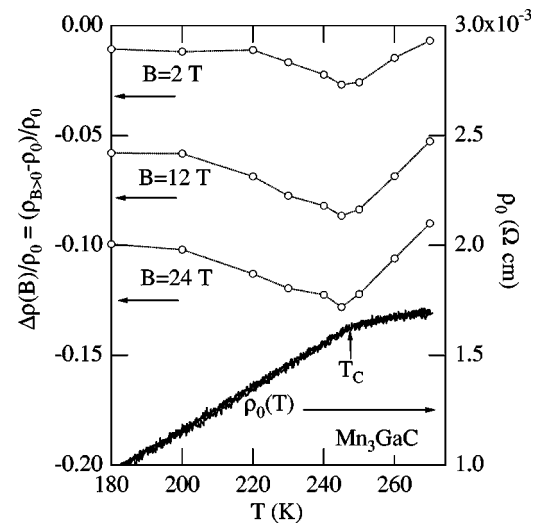


FIG. 4. Normalized magnetoresistance of Mn_3GaC in the vicinity of T_C .

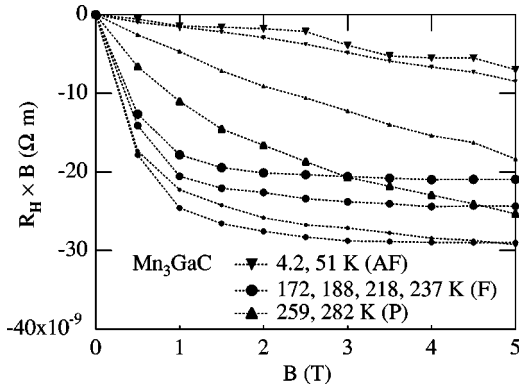


FIG. 5. Hall resistance of Mn_3GaC $R_H \times B$ at several temperatures. The larger markers represent the lower temperatures.

the dip of magnetoresistance in the vicinity of T_C . At $B = 24$ T, ρ is large below 140 K compared with what is expected from above 160 K. This fact indicates the difference between the intermediate phase and the ferromagnetic one. We can guess that the transition temperature between these phases is located between 140 and 160 K at $B = 24$ T, which is consistent with the phase diagram in Fig. 1.

Figure 5 shows the Hall resistance $\rho_H = R_H \times B$ of Mn_3GaC at several temperatures. ρ_H decreases linearly in the antiferromagnetic phase. However, an anomalous Hall effect is observed in the ferromagnetic phase at low magnetic fields, where the magnetization is not saturated. The normal Hall coefficient R_H in the ferromagnetic phase is determined by a linear fitting on the field dependence of the Hall resistance above 2 T. In the vicinity of T_C , the magnetization curves are not straight lines up to 5 T,³ so that the normal Hall coefficient R_H cannot be determined. We determined the normal Hall coefficient except for the vicinity of T_C . The temperature dependence of $1/R_H$ is shown in Fig. 6. The carriers of Mn_3GaC in the antiferromagnetic and ferromagnetic phases should be electrons since the normal Hall coefficients are negative. The values of R_H in the ferromagnetic phase are very small, which causes the dispersion of $1/R_H$. However, the average of $1/R_H$'s in the ferromagnetic phase is about five times larger than those in the antiferromagnetic phase. The values of carrier density in the antiferromagnetic

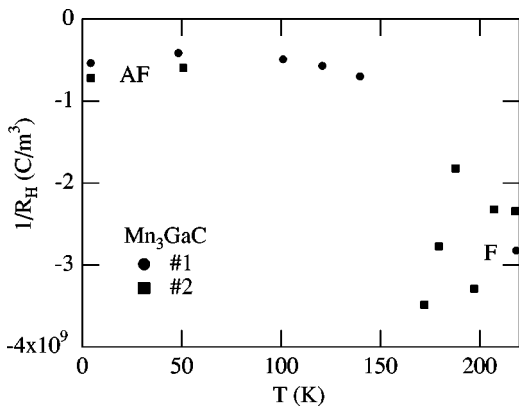


FIG. 6. Inverse of the normal Hall coefficient of Mn_3GaC at several temperatures.

and ferromagnetic phases are estimated from this result to be $0.2/\text{Mn}_3\text{GaC}$ and $\sim 1/\text{Mn}_3\text{GaC}$, respectively.

IV. DISCUSSION

First, we discuss the magnetoresistance in the vicinity of the Curie temperature. We employ a simple model used by de Gennes and Friedel,⁷ based on the following assumptions:

- (1) There is a lattice of scattering spins S_j at sites \mathbf{R}_j .
- (2) The energy of a conduction electron is expressed by $\hbar^2 \mathbf{k}^2 / 2m^*$, where $\hbar \mathbf{k}$ is the crystal momentum of the electron and m^* is its effective mass.
- (3) The interaction of a conduction electron with the array of scattering spins is simply described by $V = G \sum_j \delta(\mathbf{r} - \mathbf{R}_j) S_j s$, where \mathbf{r} and s are the position and spin operators of the conduction electron, respectively.
- (4) Inelasticity is not taken into account so that spin-flip scatterings are neglected.
- (5) The resistivity due to spin scattering is $\rho = m^* / n e^2 \tau$, where n and τ are the density of the conduction electrons and the relaxation time, respectively.

If we use the first-order perturbation theory (Fermi's golden rule), summing over all final states and employing the thermodynamical average for the initial states, we can calculate the differential scattering cross section.

$$\frac{d\sigma(\theta)}{d\Omega} = \frac{2\pi}{\sigma_0} \sum_j \Gamma(\mathbf{R}_j) \exp(i\mathbf{K} \cdot \mathbf{R}_j). \quad (1)$$

Here, $\hbar \mathbf{K}$ is the change of the momentum that depends on the elastic scattering angle θ ,

$$\sigma_0 \equiv \frac{1}{4\pi} \left(\frac{m^* G}{\hbar^2} \right)^2 S(S+1) \quad (2)$$

is the total scattering cross section per scattering at high temperatures where the spin-spin correlations are expected to be negligible, and

$$\Gamma(\mathbf{R}_j) \equiv \frac{\langle S_j \cdot S_0 \rangle - \langle S_j \rangle \cdot \langle S_0 \rangle}{S(S+1)} \quad (3)$$

is the static spin-spin correlation function for two spins separated by \mathbf{R}_j . Using the differential scattering cross section, we obtain the relaxation time by

$$\frac{\tau_0}{\tau} = \frac{2\pi}{\sigma_0} \int_0^\pi \frac{d\sigma(\theta)}{d\Omega} (1 - \cos \theta) \sin \theta d\theta. \quad (4)$$

Fisher and Langer pointed out the similarity of the formula of the relaxation time with that of Heisenberg's magnetic energy.⁸ For $T > T_C$, both are convergent sums of terms containing the same *force*-dependent factors $\Gamma(\mathbf{R})$. Therefore, they concluded

$$\frac{\partial \rho_{\text{mag}}}{\partial T} \propto C_{\text{mag}} \quad (5)$$

in a paramagnetic state, where C_{mag} is the magnetic heat capacity and ρ_{mag} is the resistivity according as the above-

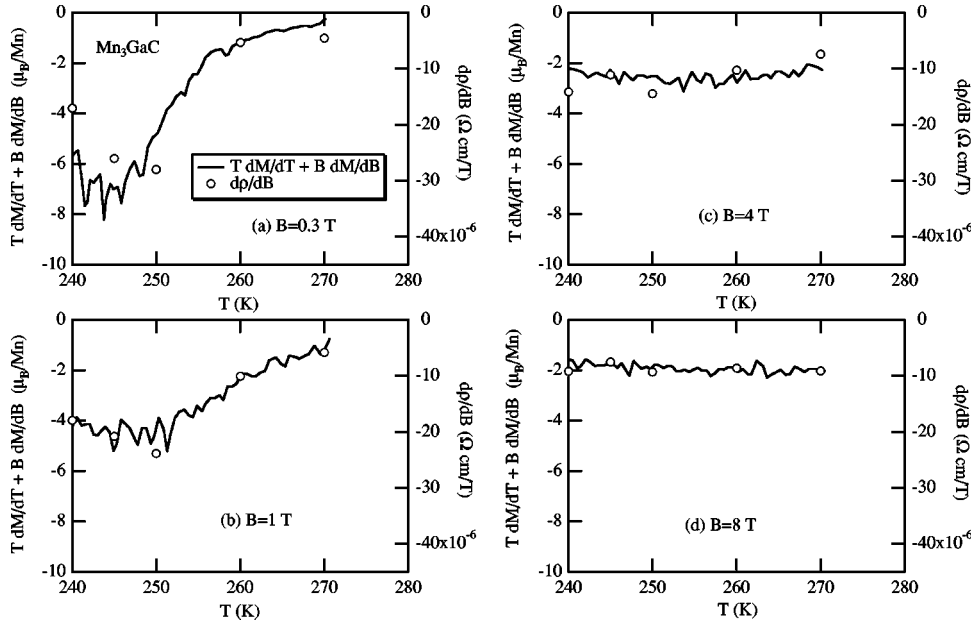


FIG. 7. The left- and the right-side values of Eq. (7) are plotted at $B=0.3$ (a), 1 (b), 4 (c), and 8 T (d) in the vicinity of T_C .

mentioned assumption (5). This formula is not so convenient in the present case, since the heat capacity due to lattice vibrations C_{lat} is much greater than C_{mag} in the temperature range that we are interested in. Therefore, we should go back to their basic idea supposing $\rho_{\text{mag}} \propto U_{\text{mag}}$. We suppose that the lattice scattering is not so much affected by the magnetic field compared with the magnetic spin motion, so

$$\frac{\partial \rho}{\partial B} \simeq \frac{\partial \rho_{\text{mag}}}{\partial B} \propto \frac{\partial U_{\text{mag}}}{\partial B}. \quad (6)$$

Dividing the thermodynamical equation of $\delta U = T \delta S + B \delta M - P \delta V$ by δB , we obtain

$$\left(\frac{\partial U}{\partial B} \right)_T = T \left(\frac{\partial M}{\partial T} \right)_B + B \left(\frac{\partial M}{\partial B} \right)_T - P \left(\frac{\partial V}{\partial B} \right)_T. \quad (7)$$

Comparing with the first term of eq. (7) in the vicinity of T_C , the second term is estimated to be much smaller than the first term by a factor of $\sim -10^{-1}$, while the third term is almost negligible ($\sim 10^{-3}$) in the ambient pressure.³ Therefore, we expect

$$\frac{\partial \rho}{\partial B} \propto T \frac{\partial M}{\partial T} + B \frac{\partial M}{\partial B}. \quad (8)$$

Using this relation, $(\partial U / \partial B)_T = T(\partial M / \partial T)_B + B(\partial M / \partial B)_T$ was calculated from the experimental results at several magnetic fields. The results are shown in Fig. 7. The relation (8) is in agreement with the experimental results for $\partial \rho / \partial B$. Thus, the magnetoresistance of Mn_3GaC in the vicinity of T_C can be well explained by the simple model where the conduction electrons are scattered by the s - d exchange interaction potential. It should be noted that the scattering spin in the s - d potential is in fact the difference from its average value. Thus the s - d potential is nothing but an ‘‘additional’’ effect, as long as the effective mass and the density of conduction electrons are clearly defined. Otherwise, this model is not applicable. Thus, from the good agreement we ob-

tained in Fig. 7, we can assume that the effective mass and the density of carriers of this compound can be well defined for the paramagnetic and ferromagnetic phases near T_C . The normal Hall coefficients in the paramagnetic phase at higher temperatures, where the magnetization curves become straight, are required to examine this possibility.

Next, we discuss the giant magnetoresistance by which the magnetic order-order transition is accompanied. The temperature dependence of the Hall coefficient of Mn_3GaC suggests that the carrier density in the ferromagnetic phase is about five times larger than that in the antiferromagnetic one.

There are some reports about the substitution effect on Mn_3GaC .^{9,10} According to them, if the Mn atoms are partly substituted by Fe or Co (or Cr), which have more (or less) electrons, the first-order transition temperature decreases (or increases). It is consistent with our experimental result of the Hall effect.

Meanwhile, the transition temperature increases if C atoms are slightly substituted for N atoms.¹¹ Therefore, we consider that this small substitution does not increase carrier densities, but gives rise to an expansion of the unit-cell volume. It indicates that the conduction electrons belong mainly to Mn. In other words, the electrons in the Mn atoms have a dominant role in the magnetic and transport properties.

Now, we return to the abrupt decrease in resistance of about 80% at 4.2 K. The ratio agrees with that in the Hall coefficient between the antiferromagnetic and ferromagnetic phases. Therefore, it can be interpreted that the jump of the resistance simply represents the change of the carrier density between the antiferromagnetic and the intermediate phase. The carrier density in the intermediate phase may be nearly the same as that in the ferromagnetic phase. Now, we consider how the carrier density depends on the magnetic states.

Yuasa *et al.*¹² reported that the resistance of Fe(Rh, Pt) changes abruptly due to a magnetic transition of the first order, and it could be explained using a model¹³ in which the s - d exchange interaction potential causes the resistance

change. In contrast with our discussion above, they consider the drastic change in the combination of S_j 's at the magnetic order-order transition to cause the change in the conduction band, the effective mass, and the density of conduction electrons. The assumption of their model is that the magnetic order-order transition does not affect the effective mass and the density of conduction electrons, *except through the s-d interaction*. Obviously, it requires that the conduction electrons and the scattering spins are distinguished in the strict sense.

In the case of Mn_3GaC , however, there is no reason to suppose the magnetic electrons do not contribute to the conductivity. Furthermore, the amplitude of the magnetic moment depends on the magnetic states, so that there is a prominent difference in the band structure between the antiferromagnetic and ferromagnetic (intermediate) states. Therefore, the model of Yuasa *et al.* does not apply to Mn_3GaC . The "magnetic-phase" dependence of the resistivity in this system should be explained by changes of magnetic scattering, the carrier density, and the effective mass.

The magnetic order-order transition observed in the present experiment is an open question. There have been models to describe such transitions. Kittel proposed an exchange-inversion model, in which two magnetic sublattices are coupled by the exchange interaction that varies with increasing volume and changes its sign at a critical point.¹⁴ Moriya and Usami also proposed another model, in which the driving force to produce the magnetic order-order transition is the situation that uniform and staggered susceptibilities obey the Curie-Weiss law due to spin fluctuations and their signs can be changed depending on temperature.¹⁵ Although the former model of Kittel is based on the localized-moment picture and the latter of Moriya and Usami is on the itinerant-electron model, these models have a common mathematical description concerning the magnetic free energy that is expanded into terms of scalar product of magnetizations and the temperature-dependent coefficients of second order pass zero to drive the system into another magnetic ordered state. These models were, however, already critically analyzed. The former model could not explain the negative pressure dependence of the first-order transition temperature.¹⁶ The latter model could not describe the first-order transition between the antiferromagnetic and intermediate states induced by applying high magnetic fields.³

In the present case, the difference between the antiferromagnetic and the ferromagnetic (intermediate) phase is not only the magnetic moment and the magnetic structure, but also the carrier density and the effective mass. Information of the electronic structure for each magnetic state is indispensable to carry out further investigation of both magnetic and

transport properties. According to band calculation for this compound,¹⁷ the density of states at the Fermi level in the antiferromagnetic state is larger than that in the ferromagnetic state. It is not consistent with our present experimental results. Furthermore, the heat capacity of $\text{Mn}_3\text{Ga}_{1-x}\text{Al}_x\text{C}$ was measured for $0 \leq x \leq 0.4$ (Ref. 18) and shows also the opposite tendency; the coefficient of the electronic specific heat in the intermediate phase $\gamma_1 \approx 30$ mJ/K²mol is higher than $\gamma_{\text{AF}} \approx 20$ mJ/K²mol in the antiferromagnetic phase. The former value is three times larger than the calculated value in the ferromagnetic state, whereas the calculated value in the antiferromagnetic state is not so different from the latter experimental one. Therefore, it is necessary to examine the band calculations in the intermediate and ferromagnetic states. Experimentally, the use of single crystals of Mn_3GaC is essential for the study of the Fermi surface of the conduction electrons in Mn_3GaC by the de Haas–van Alphen effect.

V. SUMMARY

We have measured the transverse magnetoresistance of Mn_3GaC in pulsed high magnetic fields up to 25 T. An abrupt jump in resistance has been observed at low temperatures due to the field-induced magnetic transition between the antiferromagnetic and the intermediate phase. The change ratio at 4.2 K, where the scatterings by magnetic spin fluctuations are reduced, is consistent with the ratio of the normal Hall coefficient in the antiferromagnetic phase to that in the ferromagnetic one, so that we can deduce that the giant magnetoresistance is caused by the change of carrier density between the antiferromagnetic and the intermediate phase. Since the amplitude of the magnetic moments, which may originate from the conducting *d* electrons in Mn ions, depends on magnetic states, the electron scattering by magnetic moments is not the only mechanism causing the change of the carrier density at the transition between the antiferromagnetic and ferromagnetic (intermediate) states. It is required that the electronic structure of these magnetic states is revealed by other means. The magnetoresistance in the paramagnetic phase near T_C can be explained using a simple model by de Gennes and Friedel, which takes into account only the scatterings by magnetic spins. This picture will be examined by the Hall resistivity measurements in the paramagnetic state at higher temperatures and higher magnetic fields, which will clarify whether the carrier density varies between the ferromagnetic and paramagnetic states.

ACKNOWLEDGMENT

One of the authors (K.K.) is most grateful to Professor M. Kataoka for his advice on the discussion.

*Present address: RIKEN (The Institute of Physical and Chemical Research), Wako, Saitama 351-0198, Japan.

†Present address: Hitachi Central Research Laboratory, Kokubunji, Tokyo 185-8601, Japan.

¹D. Fruchart and E. F. Bertaut, J. Phys. Soc. Jpn. **44**, 781 (1978).

²T. Kaneko and T. Kanomata, in *Recent Advance in Magnetism of Transition Metal Compounds*, edited by A. Kotani and N. Su-

zuki (World Scientific, Singapore, 1993), p. 103.

³K. Kamishima, M. I. Bartashevich, T. Goto, M. Kikuchi, and T. Kanomata, J. Phys. Soc. Jpn. **67**, 1748 (1998).

⁴D. Fruchart, E. F. Bertaut, F. Sayetat, M. Nasr Eddine, R. Fruchart, and J. P. Senateur, Solid State Commun. **8**, 91 (1970).

⁵D. Fruchart, E. F. Bertaut, B. L. Clerc, L. D. Khoi, P. Veillet, G. Lorthioir, M. E. Fruchart, and R. Fruchart, J. Solid State **8**, 182

- (1973).
- ⁶S. Takeyama, H. Ochimizu, S. Sasaki, and N. Miura, *Meas. Sci. Technol.* **3**, 662 (1992).
- ⁷P. G. de Gennes and J. Friedel, *J. Phys. Chem. Solids* **4**, 71 (1958).
- ⁸M. E. Fisher and J. S. Langer, *Phys. Rev. Lett.* **20**, 665 (1968).
- ⁹T. Kanomata, T. Harada, and T. Kaneko, in *Proceedings of the International Conference on Physics of Transition Metals, Darmstadt, 1992* (World Scientific Press, London, 1993), p. 875 [*Int. J. Mod. Phys. B* **7**, 875 (1993)].
- ¹⁰T. Harada, K. Nishimura, T. Kanomata, and T. Kaneko, *Jpn. J. Appl. Phys., Suppl.* **32-3**, 281 (1993).
- ¹¹Ph. l'Heritier, D. Boursier, and R. Fruchart, *Mater. Res. Bull.* **14**, 1203 (1979).
- ¹²S. Yuasa, T. Akiyama, H. Miyajima, and Y. Otani, *J. Phys. Soc. Jpn.* **64**, 3978 (1995).
- ¹³R. J. Elliott and F. A. Wedgwood, *Proc. Phys. Soc. London* **81**, 846 (1963).
- ¹⁴C. Kittel, *Phys. Rev.* **120**, 335 (1960).
- ¹⁵T. Moriya and K. Usami, *Solid State Commun.* **23**, 935 (1977).
- ¹⁶J. P. Bouchaud, R. Fruchart, R. Pauthenet, M. Guillot, H. Bartholin, and F. Chaisse, *J. Appl. Phys.* **37**, 971 (1966).
- ¹⁷M. Shirai, Y. Ohata, N. Suzuki, and K. Motizuki, *Jpn. J. Appl. Phys., Suppl.* **32-3**, 250 (1993).
- ¹⁸H. Wada (unpublished).